PHYSICAL REVIEW D **108,** 032007 (2023)

Search for CP violation using $\hat{T}$-odd correlations in $B^0 \to p\bar{p}K^+\pi^-$ decays

R. Aaij *et al.*[*]
(LHCb Collaboration)

(Received 19 May 2022; accepted 22 December 2022; published 8 August 2023)

A search for CP and P violation in charmless four-body $B^0 \to p\bar{p}K^+\pi^-$ decays is performed using triple-product asymmetry observables. It is based on proton-proton collision data collected by the LHCb experiment at center-of-mass energies of 7, 8 and 13 TeV, corresponding to a total integrated luminosity of 8.4 fb^{-1}. The CP- and P-violating asymmetries are measured both in the integrated phase space and in specific regions. No evidence is seen for CP violation. P-parity violation is observed at a significance of 5.8 standard deviations.

DOI: 10.1103/PhysRevD.108.032007

I. INTRODUCTION

Studying CP violation in b-hadron decays is one of the main purposes of the LHCb experiment, aimed at testing the validity of the Cabibbo-Kobayashi-Maskawa (CKM) mechanism in the Standard Model (SM). New sources of CP violation, beyond the CKM mechanism, can provide insights into the matter-antimatter asymmetry observed in the Universe. Multibody B-meson decays have proven to be an excellent laboratory for studying CP violation thanks to significant interference between the underlying amplitudes. Indeed, large CP asymmetries localized in regions of phase space of charmless three-body B-meson decays have been reported by the LHCb collaboration [1–4], including the first evidence of CP violation in the $B^+ \to p\bar{p}K^+$ decay [5]. It is therefore of great interest to search for further manifestations of CP violation in baryonic B decays, where asymmetries of up to 20% are predicted [6–8].

In this paper, a search for CP and P violation based on triple-product asymmetries [9] in the charmless region of the $B^0 \to p\bar{p}K^+\pi^-$ decay[1] is reported using proton-proton (pp) collision data collected with the LHCb detector, corresponding to a total integrated luminosity of 8.4 fb^{-1}. A data subsample of 3 fb^{-1} was collected at center-of-mass energies of 7 and 8 TeV during 2011 and 2012 (denoted run 1) while a data subsample of 5.4 fb^{-1} was collected at 13 TeV from 2016 to 2018 (denoted run 2).

The study is performed for proton-antiproton invariant mass $m_{p\bar{p}} < 2.85\ \mathrm{GeV}/c^2$, corresponding to a region below the charmonium resonances. In this region, the decay is governed mainly by tree-level $b \to u\bar{u}s$ and loop-level $b \to s\bar{u}u$ transitions, as shown in Fig. 1.

Violation of the CP symmetry can arise from the interference of these two amplitudes, whose weak-phase difference is given by $\arg(V_{ub}V_{us}^*/V_{tb}V_{ts}^*)$, and is approximately equal to the CKM angle γ in the SM [10]. However, it is noted that this work is largely exploratory since no precise SM prediction is available yet for the full phase space of the channel under study. The only prediction available refers to the $B^0 \to p\bar{p}K^{*0}$ decay channel with an expected 1% asymmetry [6].

The three-momenta of the final-state particles in the B^0 and $\bar{B}^0$ rest frame are used to build the triple-products $C_{\hat{T}}$ for B^0 and $\bar{C}_{\hat{T}}$ for $\bar{B}^0$, which are odd under the operator $\hat{T}$ that reverses the momentum of the particles, and thus acts similarly to the P-parity operator. These triple products are defined as

$$C_{\hat{T}} = \vec{p}_{K^+} \cdot (\vec{p}_{\pi^-} \times \vec{p}_p), \qquad \bar{C}_{\hat{T}} = \vec{p}_{K^-} \cdot (\vec{p}_{\pi^+} \times \vec{p}_{\bar{p}}). \quad (1)$$

where $\vec{p}$ denotes vector momentum of the final-state particle indicated in the subscript. Under the CP operator the triple product transforms as $CP(C_{\hat{T}}) = -\bar{C}_{\hat{T}}$.

The two $\hat{T}$-odd triple product asymmetries are defined as [11]

$$A_{\hat{T}} = \frac{N(C_{\hat{T}} > 0) - N(C_{\hat{T}} < 0)}{N(C_{\hat{T}} > 0) + N(C_{\hat{T}} < 0)},$$
$$\bar{A}_{\hat{T}} = \frac{\bar{N}(-\bar{C}_{\hat{T}} > 0) - \bar{N}(-\bar{C}_{\hat{T}} < 0)}{\bar{N}(-\bar{C}_{\hat{T}} > 0) + \bar{N}(-\bar{C}_{\hat{T}} < 0)}, \quad (2)$$

where N and $\bar{N}$ are the numbers of B^0 and $\bar{B}^0$ decays satisfying the requirement expressed in the corresponding parentheses.

---

[*] Full author list given at the end of the article.

[1] Charge-conjugated decays are implicitly considered throughout the text.

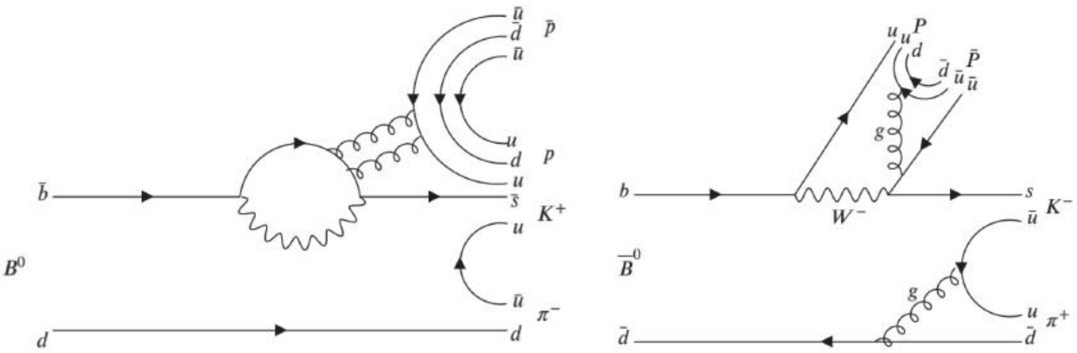

FIG. 1. Feynman diagrams for the $B^0 \to p\bar{p}K^+\pi^-$ decay in the charmless region: penguin (left) and tree (right).

The CP- and P-violating observables are then constructed as [11]

$$a_{CP}^{\hat{T}\text{-odd}} = \frac{1}{2}(A_{\hat{T}} - \bar{A}_{\hat{T}}), \qquad a_{P}^{\hat{T}\text{-odd}} = \frac{1}{2}(A_{\hat{T}} + \bar{A}_{\hat{T}}). \qquad (3)$$

A significant deviation from zero in these two observables would indicate CP violation and P violation, respectively. In contrast to the asymmetry between the phase-space integrated rates, triple-product asymmetries are sensitive to the interference of $\hat{P}$-even and $\hat{P}$-odd amplitudes and thus have a different sensitivity to strong phases [9,12]. Triple-product asymmetries have been used to search for CP violation in b -baryon decays [13,14] and in D-meson decays [15,16]. By construction, such asymmetries are largely insensitive to particle-antiparticle production and detector-induced asymmetries [15].

II. DETECTOR AND SIMULATION

The LHCb detector [17,18] is a single-arm forward spectrometer covering the pseudorapidity range $2 < \eta < 5$, designed for the study of particles containing b or c quarks. The detector includes a high-precision tracking system consisting of a silicon-strip vertex detector surrounding the pp interaction region [19], a large-area silicon-strip detector located upstream of a dipole magnet with a bending power of about 4 Tm, and three stations of silicon-strip detectors and straw drift tubes [20,21] placed downstream of the magnet. The tracking system provides a measurement of the momentum, p, of charged particles with a relative uncertainty that varies from 0.5% at low momentum to 1.0% at 200 GeV$/c$. The minimum distance of a track to a primary pp collision vertex (PV), the impact parameter (IP), is measured with a resolution of $(15 + 29/p_{\mathrm{T}})$ μm, where p_{T} is the component of the momentum transverse to the beam, in GeV$/c$. Different types of charged hadrons are distinguished using information from two ring-imaging Cherenkov detectors [22]. Photons, electrons and hadrons are identified by a calorimeter system consisting of scintillating-pad and preshower detectors, an electromagnetic and a hadronic calorimeter. Muons are identified by a system composed of alternating layers of iron and multiwire proportional chambers [23]. The online event selection is performed by a trigger [24], which consists of a hardware stage, based on information from the calorimeter and muon systems, followed by a software stage, which applies a full event reconstruction.

At the hardware trigger stage, events are required to have a muon with high p_{T} or a hadron, photon or electron with high transverse energy in the calorimeters. The software trigger requires a two-, three- or four-track secondary vertex (SV) with a significant displacement from any primary pp interaction vertex and a multivariate algorithm [25,26] is used for the identification of SVs consistent with the decay of a b hadron.

Simulation is required to model the effects of the detector acceptance and the selection requirements. Simulated $B^0 \to p\bar{p}K^+\pi^-$ decays are generated with a uniform distribution over phase space. In the simulation, pp collisions are generated using PYTHIA [27] with a specific LHCb configuration [28]. Decays of unstable particles are described by EvtGen [29], in which final-state radiation is generated using PHOTOS [30]. The interaction of the generated particles with the detector, and its response, are implemented using the Geant4 toolkit [31] as described in Ref. [32].

III. SELECTION

The $B^0 \to p\bar{p}K^+\pi^-$ candidates are formed by combining four charged hadron candidates: a proton, an antiproton, as well as a kaon and a pion of opposite electric charges. Candidates are selected using a filtering stage followed by a selection based on a boosted decision tree (BDT) classifier [33] and on particle identification (PID) requirements.

In the filtering stage, the final-state tracks are selected by requiring $p_{\mathrm{T}} > 0.3$ GeV$/c$, $p > 1.5$ GeV$/c$ and the sum of their p_{T} greater than 1.8 GeV$/c$. To ensure that the B^0 candidate is produced in the primary interaction, a tight requirement on the direction angle, θ, between the reconstructed B^0 momentum and the distance vector between the associated PV and the B^0 decay vertex is imposed

($\cos\theta > 0.9999$). Moreover, in order to exclude final-state particles coming directly from the PV, a requirement of $\chi^2_{\mathrm{IP}} > 8, 5, 3$ is imposed respectively to pion, kaon and proton candidates, where χ^2_{IP} is defined as the difference between the vertex fit χ^2 of a PV reconstructed with and without the considered track. The different χ^2_{IP} requirements reflect the different amount of background expected for each particle type.

A BDT classifier is then used to further suppress combinatorial background. The input variables are: the χ^2_{IP} and the flight distance of the B^0 candidate; the quality of the B^0 vertex; the minimum p and p_{T} between proton and antiproton; the largest distance of closest approach between any pair of tracks belonging to the signal candidate; and the pointing variable defined as $|\vec{p}_B|\sin\theta/(|\vec{p}_B|\sin\theta + \sum_i |\vec{p}_i|\sin\theta_i)$ where $\vec{p}_B$ is the momentum of the B^0 candidate, $\vec{p}_i$ is the momentum of daughter i and θ_i is the angle between $\vec{p}_i$ and the vector connecting the primary and secondary vertices.

The BDT classifier is trained using simulated $B^0 \to p\bar{p}K^+\pi^-$ decays as signal and candidates in the B^0 invariant-mass region above the signal, $5450 < m_{p\bar{p}K^+\pi^-} < 5550\ \mathrm{GeV}/c^2$, as background. Tight PID requirements are applied to suppress cross-feed background from other b-hadron decays, where one final-state particle is misidentified. An optimized combination of BDT and PID requirements is chosen in order to maximize the figure of merit $S/\sqrt{S+B}$, where $S(B)$ is the signal (background) yield, giving a signal retention of about 64% and a background rejection of more than 98%. After all selection requirements are applied, 4% of the events have multiple candidates. For these events, one candidate is chosen randomly.

To reject intermediate charm resonances, candidates with a $K^+\pi^-$ invariant mass compatible with the $\bar{D}^0$ meson mass and a $\bar{p}K^+\pi^-$ invariant mass compatible with the $\bar{\Lambda}_c^-$ baryon mass are removed. In order to exclude charmonium contributions, the $p\bar{p}$ invariant mass is required to be less than $2.85\ \mathrm{GeV}/c^2$. The vetoed candidates corresponding to the charmed $B^0 \to p\bar{p}\bar{D}^0(\to K^+\pi^-)$, which have the same final state as the signal decay, are retained as a control channel for systematic studies.

The $p\bar{p}K^+\pi^-$ invariant-mass distributions after the selection are shown in Fig. 2. A few sources of background contribute into the considered B^0 invariant-mass region and consist mainly of b-hadron decays where final-state hadrons are not correctly identified. Partially reconstructed decays are also present in the low-mass region, but do not constitute a peaking background. All these background sources are included in the baseline fit model described in Sec. IV.

IV. MEASUREMENT OF ASYMMETRIES

The asymmetries for $B^0 \to p\bar{p}K^+\pi^-$ decays are measured using an extended maximum likelihood fit to the $m_{p\bar{p}K^+\pi^-}$ distributions. The selected data sample is split into four subsamples according to the B^0 ($\bar{B}^0$) flavor and the sign of $C_{\hat{T}}$ ($\bar{C}_{\hat{T}}$). A simultaneous fit to the $m_{p\bar{p}K^+\pi^-}$ distributions of the four subsamples in Fig. 2 is used to

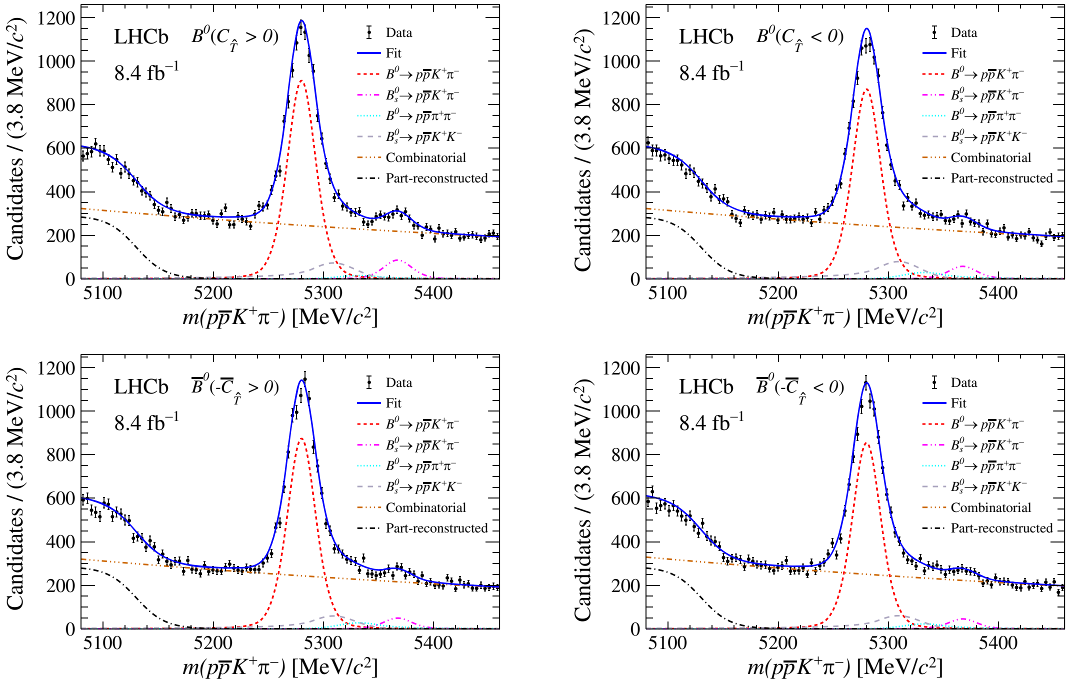

FIG. 2. Distributions for combined run 1 and run 2 data of the $p\bar{p}K^+\pi^-$ invariant mass in the four samples defined by B^0 ($\bar{B}^0$) flavor and the sign of $C_{\hat{T}}$ ($\bar{C}_{\hat{T}}$). The results of the fit, as described in the legend, are overlaid on the data.

determine the number of signal and background yields and the asymmetries $A_{\hat{T}}$ and $\bar{A}_{\hat{T}}$. The two asymmetries A_T and $\bar{A}_T$ are included in the fit model as

$$N_{B^0,C_{\hat{T}}>0} = \frac{1}{2}N_{B^0}(1 + A_{\hat{T}}), \tag{4}$$

$$N_{B^0,C_{\hat{T}}<0} = \frac{1}{2}N_{B^0}(1 - A_{\hat{T}}), \tag{5}$$

$$N_{\bar{B}^0,-\bar{C}_{\hat{T}}>0} = \frac{1}{2}N_{\bar{B}^0}(1 + \bar{A}_{\hat{T}}), \tag{6}$$

$$N_{\bar{B}^0,-\bar{C}_{\hat{T}}<0} = \frac{1}{2}N_{\bar{B}^0}(1 - \bar{A}_{\hat{T}}), \tag{7}$$

where N denotes the number of B^0 and $\bar{B}^0$ satisfying the requirement on $C_{\hat{T}}$ and $\bar{C}_{\hat{T}}$. The P- and CP-violating asymmetries, $a_P^{\hat{T}\text{-odd}}$ and $a_{CP}^{\hat{T}\text{-odd}}$, are then obtained according to Eq. (3). The correlations between the $A_{\hat{T}}$ and $\bar{A}_{\hat{T}}$ asymmetries are verified to be negligible.

The invariant-mass distributions of the $B^0 \to p\bar{p}K^+\pi^-$ and $B_s^0 \to p\bar{p}K^+\pi^-$ decays are both modeled by a Hypatia function [34], with mean and common width determined from data. All other fit parameters for these decays are taken from simulation. The two main sources of cross-feed backgrounds are due to $B^0 \to p\bar{p}K^+K^-$ and $B^0 \to p\bar{p}\pi^+\pi^-$ decays, where a kaon or a pion is misidentified. They are modeled with a double Crystal Ball function [35] with all shape parameters fixed according to simulation. The combinatorial background is parametrized with an exponential function where the parameters are left free to vary in the fits. Partially reconstructed background is described by a function of the form $f(m) = (e^{c(m-m_0)} + 1)^{-1}$, where the parameters m_0 and c are determined from data.

Two different approaches are followed to search for P and CP violation: a measurement integrated over the phase space, with the charmonium region removed, and measurements in different regions of the phase space. In multibody decays, CP asymmetries may vary over the phase space due to resonant contributions and their interference effects, possibly canceling when integrated over the whole phase space. To enhance the sensitivity to CP violation, measurements in different regions of the phase space are performed. No P-odd amplitude information from an amplitude analysis is available for the $B^0 \to p\bar{p}K^+\pi^-$ decay to provide information on the most interesting phase-space regions. The results of the first approach are obtained by fitting the phase-space integrated data sample divided according to the B flavor and the sign of the triple product. The fit result is shown in Fig. 2.

The measurements in different regions of phase space are performed by dividing the sample using a binning scheme based on the invariant masses of the $K^+\pi^-$ and $p\bar{p}$ combinations, $m_{K^+\pi^-}$ and $m_{p\bar{p}}$, the cosine of the angle of the K^+ (p) with respect to the opposite direction to the B^0 momentum in the $K^+\pi^-$ $(p\bar{p})$ rest frame, $\cos\theta_{K^+\pi^-}$ $(\cos\theta_{p\bar{p}})$, and the angle between the planes defined by the $K^+\pi^-$ and $p\bar{p}$ tracks in the B^0 rest frame, ϕ. The background-subtracted distributions of $m_{K^+\pi^-}$, $m_{p\bar{p}}$, $\cos\theta_{K^+\pi^-}$, $\cos\theta_{p\bar{p}}$, and ϕ for B^0 $(\bar{B}^0)$ candidates with $C_{\hat{T}} > 0$ and $C_{\hat{T}} < 0$ $(-\bar{C}_{\hat{T}} > 0$ and $-\bar{C}_{\hat{T}} < 0)$ are shown in Fig. 5 (Appendix B).

Two different schemes, chosen before examining the data to avoid possible biases, are used to divide the phase space. The phase space is divided into 24 (40) regions and the definition of the scheme A (B) is reported in Table II (Table IV) of Appendix A. In binning scheme B, some region edges in the $m(K^+\pi^-)$ variable correspond to the resonance mass pole where the strong phase changes sign. This choice further enhances the sensitivity to CP violation. Because of many overlapping resonances in the $K^+\pi^-$ mass spectrum, only the $K^*(892)^0$ and $K_2^*(1430)$ states, for which the peaks can be clearly identified, are split.

The same fit model used for the integrated measurement is exploited to fit the B^0 mass distribution separately for each phase-space region. The distributions of the measured asymmetries for scheme A (B) are shown in Fig. 3 (Fig. 4) and the numerical results are reported in Table III (Table V) in Appendix A.

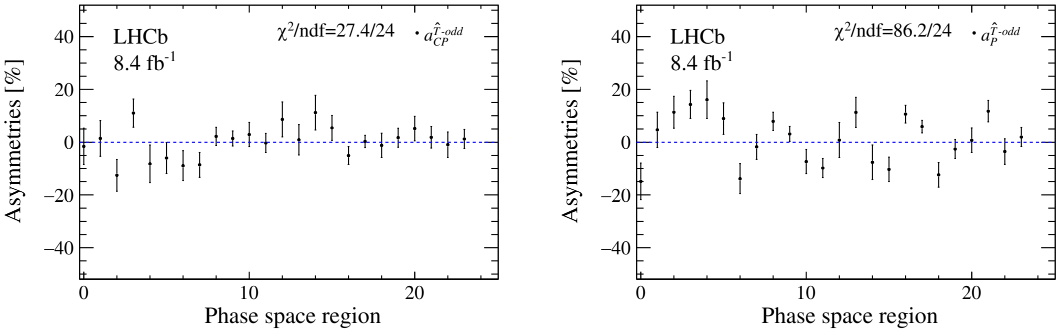

FIG. 3. The $a_{CP}^{\hat{T}\text{-odd}}$ (left) and $a_P^{\hat{T}\text{-odd}}$ (right) asymmetry parameters in each region of the phase space for run 1 and run 2 data combined for binning scheme A. The error bars represent the sum in quadrature of the statistical and systematic uncertainties. The χ^2 per number of degrees of freedom (ndf) is calculated with respect to the null hypothesis.

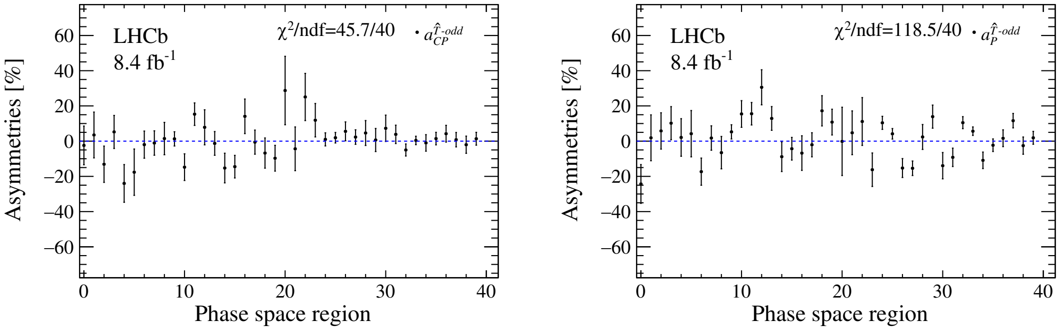

FIG. 4. The $a_{CP}^{\hat{T}\text{-odd}}$ (left) and $a_{P}^{\hat{T}\text{-odd}}$ (right) asymmetry parameters in each region of the phase space for run 1 and run 2 data combined for binning scheme B. The error bars represent the sum in quadrature of the statistical and systematic uncertainties. The χ^2 per ndf is calculated with respect to the null hypothesis.

The compatibility with the *CP* (*P*) conservation hypothesis is tested by means of a χ^2 test, where the χ^2 is defined as $X^T V^{-1} X$, with X denoting the array of $a_{CP}^{\hat{T}\text{-odd}}$ ($a_{P}^{\hat{T}\text{-odd}}$) measurements, V^{-1} is the inverse of the covariance matrix V, defined as the sum of the statistical and systematic covariance matrices. An average systematic uncertainty, whose evaluation is discussed in Sec. V, is assumed for each bin. The statistical and systematic uncertainties are considered uncorrelated among the bins. No significant *CP* violation is observed with either of the binning schemes, while some phase-space regions exhibit *P* violation.

V. SYSTEMATIC UNCERTAINTIES AND CROSS-CHECKS

The systematic uncertainties are determined in each phase space region with simulated pseudoexperiments having the same number of signal candidates as the real data and the largest value found in a single bin is used as the systematic error representative for all bins. The sources of systematic uncertainty and their relative contributions, expressed as a percentage of the statistical uncertainty, are listed in Table I.

TABLE I. Sources of systematic uncertainty and their relative contributions expressed as a percentage of the statistical uncertainty. In order to obtain the absolute systematic uncertainty assigned to a specific region of the phase space, the numbers reported here have to be multiplied by the corresponding statistical uncertainties. $\Delta a_{CP}^{\hat{T}\text{-odd}}$ and $\Delta a_{P}^{\hat{T}\text{-odd}}$ indicate the uncertainty assigned to $a_{CP}^{\hat{T}\text{-odd}}$ and $a_{P}^{\hat{T}\text{-odd}}$, respectively.

Contribution	$\Delta a_{CP}^{\hat{T}\text{-odd}}[\%]$	$\Delta a_{P}^{\hat{T}\text{-odd}}[\%]$
Detector resolution	1	1
Fit procedure	5	5
Alternative fit	5	5
Mass resolution	5	5
Total	9	9

The contributions are uncorrelated and thus added in quadrature. The systematic uncertainty related to the detector resolution, which could introduce a migration of signal decays between $C_{\hat{T}} > 0$ and $C_{\hat{T}} < 0$ ($-\bar{C}_{\hat{T}} > 0$ and $-\bar{C}_{\hat{T}} < 0$) categories for B^0 ($\bar{B}^0$), is estimated in every region of the phase space using a simulated sample of $B^0 \to p\bar{p}K^+\pi^-$ decays. The difference between the reconstructed and generated asymmetry is considered as systematic uncertainty. Although the difference is negligibly small, a common relative uncertainty of 1% is assigned to every phase space region. To test whether the fit procedure introduces any bias, pseudoexperiments are generated from the baseline fit model using the measured asymmetry values and fitting them with the same model. Since the observed bias is compatible with zero, the largest value among the mean of the pull distribution estimated in every single region of the phase space, 5%, is assigned as the fit procedure relative systematic uncertainty. The systematic uncertainties related to the choice of the model for the signal and background components are evaluated by using alternative models that have comparable fit quality with the baseline model. A double Crystal Ball function is used for the signal while the background is described by a linear function. Pseudoexperiments are generated using the alternative model and the baseline fit model is then used to fit each generated sample. Since the observed bias is not significantly different from zero, the largest value among the mean of the pull distribution estimated in every single region of the phase space, 5%, is assigned as alternative fit model systematic uncertainty. The effect of fixing the mass and resolutions of the cross-feed background from simulated samples is assessed by varying their values. The mass and the resolution are varied uniformly in a ± 3 and ± 5 MeV/c^2 range, respectively, around the values found in the simulation. The range is chosen in order to take into account the possible discrepancy between simulation and data for the B^0 mass and resolution. A relative contribution of 5%, which corresponds to the largest value among the mean of the pull distribution estimated in every single region of the phase space, is assigned as systematic uncertainty. As a cross-check, a possible experimental bias is tested by measuring the $a_{CP}^{\hat{T}\text{-odd}}$ asymmetry using the $B^0 \to p\bar{p}\bar{D}^0(\to K^+\pi^-)$ control channel. Since negligible CP violation is expected for this channel, which proceeds through the tree-level $b \to cu\bar{u}$ transition, any deviation of the CP asymmetry from zero is considered as a bias introduced by the experimental reconstruction and analysis technique. The asymmetry measured on the $B^0 \to p\bar{p}\bar{D}^0(\to K^+\pi^-)$ control sample, $a_{CP}^{\hat{T}\text{-odd}} = (-1.0 \pm 1.5)\%$, shows no significant bias. The test is repeated for different regions of phase space, using a control sample weighted according to the kinematic distributions of the signal and for different magnet polarities, and gives consistent results. Further cross-checks are made to test the stability of the results with respect to the different magnet polarities, the choice made in the selection of multiple candidates, and the effect of the trigger and selection criteria. No systematic uncertainty is assigned since all these checks give results compatible with the nominal ones. In addition, correlations between $C_{\hat{T}}$ and $\bar{C}_{\hat{T}}$ and the kinematic and topological variables used in the selection are checked using both simulated samples and background-subtracted data and found to be negligible.

VI. RESULTS AND CONCLUSION

In conclusion, a search for P and CP violation in $B^0 \to p\bar{p}K^+\pi^-$ decays is performed both globally and in regions of the phase space. The measured phase-space integrated asymmetries are

$$a_P^{\hat{T}\text{-odd}} = (1.49 \pm 0.85 \pm 0.08)\%,$$
$$a_{CP}^{\hat{T}\text{-odd}} = (0.51 \pm 0.85 \pm 0.08)\%,$$

where the uncertainties are respectively statistical and systematic. Both are consistent with P and CP conservation. The 1% theoretical prediction discussed in Sec. I is beyond the reach of the current experimental sensitivity. However, an observation of CP violation in the $B^0 \to p\bar{p}K^+\pi^-$ decay would have been a hint of beyond Standard Model contributions. Measurements in regions of the phase space are consistent with the CP-symmetry hypothesis with a p value of 0.28 (0.24), according to $\chi^2 = 27.4/24$ ($\chi^2 = 45.7/40$), corresponding to 1.1σ (1.2σ) deviation for scheme A (scheme B). For P symmetry, a p value of 6.1×10^{-9} (1.1×10^{-9}) is found, according to $\chi^2 = 86.2/24$ ($\chi^2 = 118.5/40$), corresponding to 5.8σ (6.0σ) deviation for scheme A (scheme B). Significant P asymmetries are observed in the region of low $p\bar{p}$ mass and near the $K^*(892)^0$ resonance. However, a full amplitude analysis of the $B^0 \to p\bar{p}K^+\pi^-$ decay is needed to associate the observed P-parity violation with any underlying resonance amplitude. In conclusion, the data are consistent with P-parity violation, but show no evidence for CP violation.

ACKNOWLEDGMENTS

We express our gratitude to our colleagues in the CERN accelerator departments for the excellent performance of the LHC. We thank the technical and administrative staff at the LHCb institutes. We acknowledge support from CERN and from the national agencies: CAPES, CNPq, FAPERJ and FINEP (Brazil); MOST and NSFC (China); CNRS/IN2P3 (France); BMBF, DFG and MPG (Germany); INFN (Italy); NWO (Netherlands); MNiSW and NCN (Poland); MEN/IFA (Romania); MICINN (Spain); SNSF and SER (Switzerland); NASU (Ukraine); STFC (United Kingdom); DOE NP and NSF (USA). We acknowledge the computing resources that are provided by CERN, IN2P3 (France), KIT and DESY (Germany), INFN (Italy), SURF (Netherlands), PIC (Spain), GridPP (United Kingdom), CSCS (Switzerland), IFIN-HH (Romania), CBPF (Brazil), Polish WLCG (Poland) and NERSC (USA). We are indebted to the communities behind the multiple open-source software packages on which we depend. Individual groups or members have received support from ARC and ARDC (Australia); Minciencias (Colombia); AvH Foundation (Germany); EPLANET, Marie Skłodowska-Curie Actions and ERC (European Union); A*MIDEX, ANR, IPhU and Labex P2IO, and Région Auvergne-Rhône-Alpes (France); Key Research Program of Frontier Sciences of CAS, CAS PIFI, CAS CCEPP, Fundamental Research Funds for the Central Universities, and Science and Technology Program of Guangzhou (China); GVA, XuntaGal, GENCAT and Prog. Atracción Talento, CM (Spain); SRC (Sweden); the Leverhulme Trust, the Royal Society and UKRI (United Kingdom).

APPENDIX A: MEASURED ASYMMETRIES IN REGIONS OF PHASE SPACE

The definitions of the regions of phase space of the four-body $B^0 \to p\bar{p}K^+\pi^-$ decay of the two binning schemes are reported in Tables II and IV. The corresponding measured asymmetries in each region of phase space are reported in Tables III and V.

TABLE II. Definition of the 24 regions that form scheme A for the $B^0 \to p\bar{p}K^+\pi^-$ decay.

Region	$m_{p\bar{p}}$ (MeV/c^2)	$m_{K^+\pi^-}$ (MeV/c^2)	$\cos\theta_{p\bar{p}}$	$\cos\theta_{K^+\pi^-}$	ϕ
0	(1800, 2850)	(500, 1200)	$(-1, 0)$	$(-1, 0)$	$(0, \pi/2)$
1	(1800, 2850)	(500, 1200)	$(-1, 0)$	$(-1, 0)$	$(\pi/2, \pi)$
2	(1800, 2850)	(500, 1200)	$(-1, 0)$	(0, 1)	$(0, \pi/2)$
3	(1800, 2850)	(500, 1200)	$(-1, 0)$	(0, 1)	$(\pi/2, \pi)$
4	(1800, 2850)	(500, 1200)	(0, 1)	$(-1, 0)$	$(0, \pi/2)$
5	(1800, 2850)	(500, 1200)	(0, 1)	$(-1, 0)$	$(\pi/2, \pi)$
6	(1800, 2850)	(500, 1200)	(0, 1)	(0, 1)	$(0, \pi/2)$
7	(1800, 2850)	(500, 1200)	(0, 1)	(0, 1)	$(\pi/2, \pi)$
8	(1800, 2850)	(1200, 2200)	$(-1, 0)$	$(-1, 0)$	$(0, \pi/2)$
9	(1800, 2850)	(1200, 2200)	$(-1, 0)$	$(-1, 0)$	$(\pi/2, \pi)$
10	(1800, 2850)	(1200, 2200)	$(-1, 0)$	(0, 1)	$(0, \pi/2)$
11	(1800, 2850)	(1200, 2200)	$(-1, 0)$	(0, 1)	$(\pi/2, \pi)$
12	(1800, 2850)	(1200, 2200)	(0, 1)	$(-1, 0)$	$(0, \pi/2)$
13	(1800, 2850)	(1200, 2200)	(0, 1)	$(-1, 0)$	$(\pi/2, \pi)$
14	(1800, 2850)	(1200, 2200)	(0, 1)	(0, 1)	$(0, \pi/2)$
15	(1800, 2850)	(1200, 2200)	(0, 1)	(0, 1)	$(\pi/2, \pi)$
16	(1800, 2850)	(2200, 3600)	$(-1, 0)$	$(-1, 0)$	$(0, \pi/2)$
17	(1800, 2850)	(2200, 3600)	$(-1, 0)$	$(-1, 0)$	$(\pi/2, \pi)$
18	(1800, 2850)	(2200, 3600)	$(-1, 0)$	(0, 1)	$(0, \pi/2)$
19	(1800, 2850)	(2200, 3600)	$(-1, 0)$	(0, 1)	$(\pi/2, \pi)$
20	(1800, 2850)	(2200, 3600)	(0, 1)	$(-1, 0)$	$(0, \pi/2)$
21	(1800, 2850)	(2200, 3600)	(0, 1)	$(-1, 0)$	$(\pi/2, \pi)$
22	(1800, 2850)	(2200, 3600)	(0, 1)	(0, 1)	$(0, \pi/2)$
23	(1800, 2850)	(2200, 3600)	(0, 1)	(0, 1)	$(\pi/2, \pi)$

TABLE III. Measurements of $a_{CP}^{\hat{T}\text{-odd}}$ and $a_{P}^{\hat{T}\text{-odd}}$ in specific phase-space regions for the $B^0 \to p\bar{p}K^+\pi^-$ decay for binning scheme A. Each value is obtained through an independent fit to the B^0 invariant-mass distribution of the candidates in the corresponding region of the phase space. The uncertainties are only statistical.

Region	$A_{\hat{T}}(\%)$	$\bar{A}_{\hat{T}}(\%)$	$a_{CP}^{\hat{T}\text{-odd}}(\%)$	$a_{P}^{\hat{T}\text{-odd}}(\%)$
0	-16.5 ± 10.1	-13.2 ± 9.5	-1.6 ± 7.0	-14.9 ± 7.0
1	6.1 ± 9.2	3.2 ± 9.8	1.4 ± 6.7	4.7 ± 6.7
2	-1.2 ± 7.0	23.9 ± 10.0	-12.5 ± 6.0	11.4 ± 6.0
3	25.3 ± 7.2	3.2 ± 7.8	11.0 ± 5.3	14.3 ± 5.3
4	7.8 ± 11.1	24.3 ± 9.0	-8.2 ± 7.1	16.1 ± 7.1
5	2.9 ± 8.3	14.9 ± 8.6	-6.0 ± 6.0	8.9 ± 5.9
6	-22.8 ± 7.4	-4.9 ± 8.6	-8.9 ± 5.7	-13.9 ± 5.7
7	-10.4 ± 6.8	6.8 ± 6.6	-8.6 ± 4.7	-1.8 ± 4.7
8	10.1 ± 5.0	5.7 ± 4.9	2.2 ± 3.5	7.9 ± 3.5
9	4.5 ± 4.0	1.7 ± 4.0	1.4 ± 2.8	3.1 ± 2.8
10	-4.5 ± 6.5	-10.2 ± 6.5	2.9 ± 4.6	-7.4 ± 4.6
11	-10.1 ± 5.2	-9.5 ± 5.2	-0.3 ± 3.7	-9.8 ± 3.7
12	9.4 ± 9.2	-7.8 ± 9.5	8.6 ± 6.6	0.8 ± 6.6
13	12.2 ± 8.2	10.4 ± 8.0	0.9 ± 5.7	11.3 ± 5.7
14	3.6 ± 9.8	-18.8 ± 8.7	11.2 ± 6.6	-7.6 ± 6.6
15	-4.9 ± 6.0	-15.7 ± 7.1	5.4 ± 4.7	-10.3 ± 4.7
16	5.5 ± 4.8	15.7 ± 4.7	-5.1 ± 3.4	10.6 ± 3.4
17	6.2 ± 3.4	5.6 ± 3.3	0.3 ± 2.4	5.9 ± 2.4
18	-13.6 ± 6.7	-11.2 ± 6.4	-1.2 ± 4.6	-12.4 ± 4.6
19	-0.9 ± 5.1	-4.3 ± 5.1	1.7 ± 3.6	-2.6 ± 3.6
20	5.9 ± 6.2	-4.4 ± 6.9	5.2 ± 4.7	0.7 ± 4.7
21	13.6 ± 5.6	9.9 ± 5.8	1.8 ± 4.0	11.7 ± 4.0
22	-4.5 ± 6.9	-2.6 ± 6.6	-0.9 ± 4.8	-3.5 ± 4.8
23	3.1 ± 5.0	0.7 ± 5.2	1.2 ± 3.6	1.9 ± 3.6

TABLE IV. Definition of the 40 regions that form scheme B for the $B^0 \to p\bar{p}K^+\pi^-$ decay.

Region	$m_{p\bar{p}}$ (MeV/c^2)	$m_{K^+\pi^-}$ (MeV/c^2)	$\cos\theta_{p\bar{p}}$	$\cos\theta_{K^+\pi^-}$	ϕ
0	(1800, 2850)	(500, 892)	$(-1,0)$	$(-1,0)$	$(0,\pi/2)$
1	(1800, 2850)	(500, 892)	$(-1,0)$	$(-1,0)$	$(\pi/2,\pi)$
2	(1800, 2850)	(500, 892)	$(-1,0)$	(0, 1)	$(0,\pi/2)$
3	(1800, 2850)	(500, 892)	$(-1,0)$	(0, 1)	$(\pi/2,\pi)$
4	(1800, 2850)	(500, 892)	(0, 1)	$(-1,0)$	$(0,\pi/2)$
5	(1800, 2850)	(500, 892)	(0, 1)	$(-1,0)$	$(\pi/2,\pi)$
6	(1800, 2850)	(500, 892)	(0, 1)	(0, 1)	$(0,\pi/2)$
7	(1800, 2850)	(500, 892)	(0, 1)	(0, 1)	$(\pi/2,\pi)$
8	(1800, 2850)	(892, 1200)	$(-1,0)$	$(-1,0)$	$(0,\pi/2)$
9	(1800, 2850)	(892, 1200)	$(-1,0)$	$(-1,0)$	$(\pi/2,\pi)$
10	(1800, 2850)	(892, 1200)	$(-1,0)$	(0, 1)	$(0,\pi/2)$
11	(1800, 2850)	(892, 1200)	$(-1,0)$	(0, 1)	$(\pi/2,\pi)$
12	(1800, 2850)	(892, 1200)	(0, 1)	$(-1,0)$	$(0,\pi/2)$
13	(1800, 2850)	(892, 1200)	(0, 1)	$(-1,0)$	$(\pi/2,\pi)$
14	(1800, 2850)	(892, 1200)	(0, 1)	(0, 1)	$(0,\pi/2)$
15	(1800, 2850)	(892, 1200)	(0, 1)	(0, 1)	$(\pi/2,\pi)$
16	(1800, 2850)	(1200, 1430)	$(-1,0)$	$(-1,0)$	$(0,\pi/2)$
17	(1800, 2850)	(1200, 1430)	$(-1,0)$	$(-1,0)$	$(\pi/2,\pi)$
18	(1800, 2850)	(1200, 1430)	$(-1,0)$	(0, 1)	$(0,\pi/2)$
19	(1800, 2850)	(1200, 1430)	$(-1,0)$	(0, 1)	$(\pi/2,\pi)$
20	(1800, 2850)	(1200, 1430)	(0, 1)	$(-1,0)$	$(0,\pi/2)$
21	(1800, 2850)	(1200, 1430)	(0, 1)	$(-1,0)$	$(\pi/2,\pi)$
22	(1800, 2850)	(1200, 1430)	(0, 1)	(0, 1)	$(0,\pi/2)$
23	(1800, 2850)	(1200, 1430)	(0, 1)	(0, 1)	$(\pi/2,\pi)$
24	(1800, 2850)	(1430, 2200)	$(-1,0)$	$(-1,0)$	$(0,\pi/2)$
25	(1800, 2850)	(1430, 2200)	$(-1,0)$	$(-1,0)$	$(\pi/2,\pi)$
26	(1800, 2850)	(1430, 2200)	$(-1,0)$	(0, 1)	$(0,\pi/2)$
27	(1800, 2850)	(1430, 2200)	$(-1,0)$	(0, 1)	$(\pi/2,\pi)$
28	(1800, 2850)	(1430, 2200)	(0, 1)	$(-1,0)$	$(0,\pi/2)$
29	(1800, 2850)	(1430, 2200)	(0, 1)	$(-1,0)$	$(\pi/2,\pi)$
30	(1800, 2850)	(1430, 2200)	(0, 1)	(0, 1)	$(0,\pi/2)$
31	(1800, 2850)	(1430, 2200)	(0, 1)	(0, 1)	$(\pi/2,\pi)$
32	(1800, 2850)	(2200, 3600)	$(-1,0)$	$(-1,0)$	$(0,\pi/2)$
33	(1800, 2850)	(2200, 3600)	$(-1,0)$	$(-1,0)$	$(\pi/2,\pi)$
34	(1800, 2850)	(2200, 3600)	$(-1,0)$	(0, 1)	$(0,\pi/2)$
35	(1800, 2850)	(2200, 3600)	$(-1,0)$	(0, 1)	$(\pi/2,\pi)$
36	(1800, 2850)	(2200, 3600)	(0, 1)	$(-1,0)$	$(0,\pi/2)$
37	(1800, 2850)	(2200, 3600)	(0, 1)	$(-1,0)$	$(\pi/2,\pi)$
38	(1800, 2850)	(2200, 3600)	(0, 1)	(0, 1)	$(0,\pi/2)$
39	(1800, 2850)	(2200, 3600)	(0, 1)	(0, 1)	$(\pi/2,\pi)$

TABLE V. Measurements of $a_{CP}^{\hat{T}\text{-odd}}$ and $a_{P}^{\hat{T}\text{-odd}}$ in specific phase-space regions for the $B^0 \to p\bar{p}K^+\pi^-$ decay for binning scheme B. Each value is obtained through an independent fit to the B^0 invariant-mass distribution of the candidates in the corresponding region of the phase space.

Region	$A_{\hat{T}}(\%)$	$\bar{A}_{\hat{T}}(\%)$	$a_{CP}^{\hat{T}\text{-odd}}(\%)$	$a_{P}^{\hat{T}\text{-odd}}(\%)$
0	-26.7 ± 17.8	-21.9 ± 12.9	-2.4 ± 11.0	-24.3 ± 11.0
1	5.4 ± 15.8	-1.6 ± 20.7	3.5 ± 13.0	1.9 ± 13.0
2	-7.3 ± 11.1	18.9 ± 17.4	-13.1 ± 10.3	5.8 ± 10.3
3	15.4 ± 12.8	5.0 ± 13.7	5.2 ± 9.4	10.2 ± 9.4
4	-21.9 ± 13.9	26.1 ± 16.3	-24.0 ± 10.7	2.1 ± 10.7
5	-13.4 ± 13.9	21.9 ± 22.3	-17.6 ± 13.1	4.2 ± 13.1
6	-19.3 ± 10.4	-15.3 ± 11.4	-2.0 ± 7.7	-17.3 ± 7.7
7	0.7 ± 10.9	2.8 ± 8.4	-1.1 ± 6.9	1.8 ± 6.9
8	-5.1 ± 12.8	-8.0 ± 13.2	1.5 ± 9.2	-6.5 ± 9.2
9	6.6 ± 5.8	4.0 ± 5.6	1.3 ± 4.0	5.3 ± 4.0
10	0.7 ± 9.0	30.2 ± 12.2	-14.8 ± 7.6	15.4 ± 7.6
11	30.9 ± 8.7	0.2 ± 9.4	15.3 ± 6.4	15.6 ± 6.4
12	38.4 ± 16.8	22.7 ± 10.7	7.9 ± 10.0	30.58 ± 9.96
13	11.6 ± 10.2	14.2 ± 8.8	-1.3 ± 6.7	12.9 ± 6.7
14	-24.1 ± 10.5	6.4 ± 13.2	-15.3 ± 8.4	-8.8 ± 8.4
15	-18.8 ± 8.6	10.2 ± 9.5	-14.5 ± 6.4	-4.3 ± 6.4
16	7.3 ± 11.9	-20.9 ± 15.6	14.1 ± 9.8	-6.8 ± 9.8
17	-2.6 ± 10.4	-1.5 ± 9.0	-0.5 ± 6.9	-2.1 ± 6.9
18	10.5 ± 11.7	24.0 ± 12.6	-6.8 ± 8.6	17.2 ± 8.6
19	1.1 ± 10.9	20.5 ± 9.8	-9.7 ± 7.3	10.8 ± 7.3
20	28.6 ± 32.0	-28.9 ± 21.9	28.7 ± 19.4	-0.1 ± 19.4
21	0.4 ± 19.3	9.1 ± 15.6	-4.4 ± 12.4	4.7 ± 12.4
22	36.2 ± 19.0	-13.9 ± 19.2	25.1 ± 13.4	11.1 ± 13.6
23	-4.3 ± 12.5	-28.1 ± 14.3	11.9 ± 9.5	-16.2 ± 9.5
24	11.4 ± 5.4	9.4 ± 5.1	1.0 ± 3.7	10.4 ± 3.7
25	6.1 ± 4.2	2.2 ± 4.3	1.9 ± 3.0	4.2 ± 3.0
26	-9.7 ± 7.6	-20.8 ± 7.6	5.6 ± 5.4	-15.3 ± 5.4
27	-13.1 ± 5.9	-17.7 ± 5.8	2.3 ± 4.1	-15.4 ± 4.1
28	7.0 ± 9.5	-2.2 ± 10.5	4.6 ± 7.1	2.4 ± 7.1
29	14.6 ± 8.9	13.3 ± 9.6	0.6 ± 6.5	13.9 ± 6.5
30	-6.6 ± 11.4	-21.2 ± 9.7	7.3 ± 7.5	-13.9 ± 7.5
31	-5.3 ± 6.7	-13.0 ± 8.0	3.8 ± 5.2	-9.2 ± 5.2
32	5.5 ± 4.8	15.5 ± 4.8	-5.0 ± 3.4	10.5 ± 3.4
33	6.1 ± 3.4	5.3 ± 3.4	0.4 ± 2.4	5.7 ± 2.4
34	-11.9 ± 6.7	-9.9 ± 6.5	-1.0 ± 4.7	-10.9 ± 4.7
35	-0.9 ± 5.1	-3.8 ± 5.0	1.4 ± 3.6	-2.3 ± 3.6
36	5.9 ± 6.3	-2.6 ± 7.1	4.2 ± 4.8	1.6 ± 4.8
37	12.4 ± 5.7	10.8 ± 5.9	0.8 ± 4.1	11.6 ± 4.1
38	-4.6 ± 7.1	-0.5 ± 6.8	-2.0 ± 4.9	-2.5 ± 4.9
39	3.3 ± 5.0	0.5 ± 5.3	1.4 ± 3.6	1.9 ± 3.6

APPENDIX B: BACKGROUND-SUBTRACTED PHASE SPACE DISTRIBUTIONS

The background-subtracted distributions of $m_{p\bar{p}}$, $m_{K^+\pi^-}$, $\cos\theta_{p\bar{p}}$, $\cos\theta_{K^+\pi^-}$ and ϕ obtained using the *sPlot* technique [36] for B^0 ($\bar{B}^0$) with $C_{\hat{T}} > 0$ and $C_{\hat{T}} < 0$ ($-\bar{C}_{\hat{T}} > 0$ and $-\bar{C}_{\hat{T}} < 0$) of the $B^0 \to p\bar{p}K^+\pi^-$ decay are shown in Fig. 5 for the combined data.

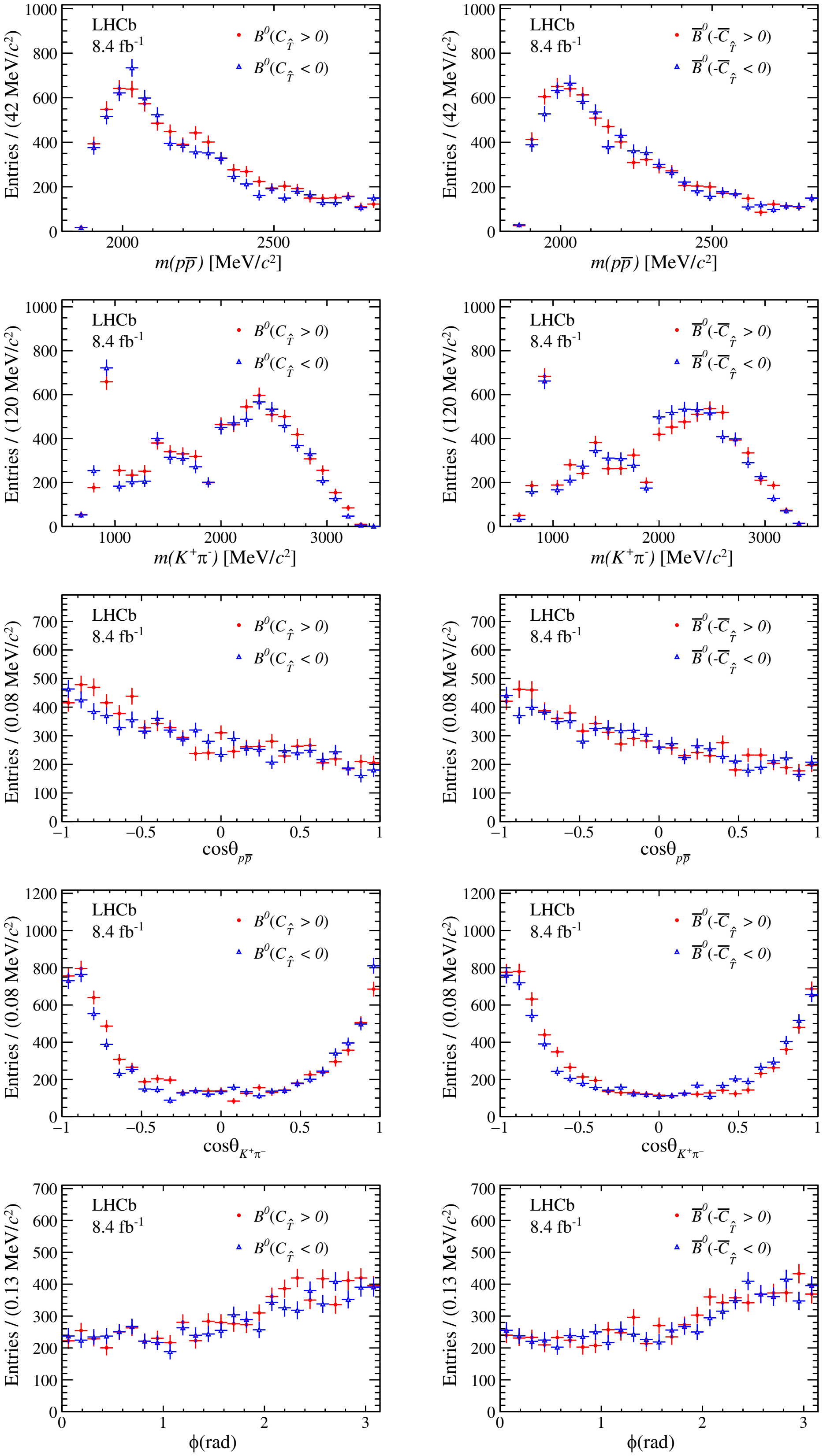

FIG. 5. Background-subtracted distributions of B^0 ($\bar{B}^0$) candidates in the variables $m_{p\bar{p}}$, $m_{K^+\pi^-}$, $\cos\theta_{p\bar{p}}$, $\cos\theta_{K^+\pi^-}$, and ϕ with $C_{\hat{T}} > 0$ and $C_{\hat{T}} < 0$ ($-\bar{C}_{\hat{T}} > 0$ and $-\bar{C}_{\hat{T}} < 0$).

[1] R. Aaij *et al.* (LHCb Collaboration), Amplitude analysis of the $B^+ \to \pi^+\pi^+\pi^-$ decay, Phys. Rev. D **101**, 012006 (2020).

[2] R. Aaij *et al.* (LHCb Collaboration), Amplitude Analysis of $B^\pm \to \pi^\pm K^+ K^-$ Decays, Phys. Rev. Lett. **123**, 231802 (2019).

[3] R. Aaij *et al.* (LHCb Collaboration), Measurement of CP Violation in the Phase Space of $B^\pm \to K^+K^-\pi^\pm$ and $B^\pm \to \pi^+\pi^-\pi^\pm$ Decays, Phys. Rev. Lett. **112**, 011801 (2014).

[4] R. Aaij *et al.* (LHCb Collaboration), Measurement of CP Violation in the Phase Space of $B^\pm \to K^\pm\pi^+\pi^-$ and $B^\pm \to K^\pm K^+ K^-$ Decays, Phys. Rev. Lett. **111**, 101801 (2013).

[5] R. Aaij *et al.* (LHCb Collaboration), Evidence for CP Violation in $B^+ \to p\bar{p}K^+$ Decays, Phys. Rev. Lett. **113**, 141801 (2014).

[6] C. Q. Geng and Y. K. Hsiao, Direct CP and T violation in B decays, Int. J. Mod. Phys. A **23**, 3290 (2008).

[7] C. Q. Geng, Y. K. Hsiao, and J. N. Ng, Direct CP Violation in $B^\mp \to p\bar{p}K^{(*)\pm}$, Phys. Rev. Lett. **98**, 011801 (2007).

[8] Y. K. Hsiao, S.-Y. Tsai, and E. Rodrigues, Direct CP violation in internal W-emission dominated baryonic B decays, Eur. Phys. J. C **80**, 565 (2020).

[9] G. Durieux and Y. Grossman, Probing CP violation systematically in differential distributions, Phys. Rev. D **92**, 076013 (2015).

[10] M. Gronau and J. L. Rosner, Triple product asymmetries in Λ_b and Ξ_b decays, Phys. Lett. B **749**, 104 (2015).

[11] A. Datta and D. London, Triple-product correlations in $B \to V_1V_2$ decays and new physics, Int. J. Mod. Phys. A **19**, 2505 (2004).

[12] G. Valencia, Angular correlations in the decay $B \to VV$ and CP violation, Phys. Rev. D **39**, 3339 (1989).

[13] R. Aaij *et al.* (LHCb Collaboration), Search for CP violation using triple product asymmetries in $\Lambda_b^0 \to pK^-\pi^+\pi^-$, $\Lambda_b^0 \to pK^-K^+K^-$, and $\Xi_b^0 \to pK^-K^-\pi^+$ decays, J. High Energy Phys. 08 (2018) 039.

[14] R. Aaij *et al.* (LHCb Collaboration), Search for CP violation and observation of P violation in $\Lambda_b^0 \to p\pi^-\pi^+\pi^-$ decays, Phys. Rev. D **102**, 051101 (2020).

[15] R. Aaij *et al.* (LHCb Collaboration), Search for CP violation using T-odd correlations in $D^0 \to K^+K^-\pi^+\pi^-$ decays, J. High Energy Phys. 10 (2014) 005.

[16] R. Aaij *et al.* (LHCb Collaboration), Search for CP violation in the phase space of $D^0 \to \pi^+\pi^-\pi^+\pi^-$ decays, Phys. Lett. B **769**, 345 (2017).

[17] A. A. Alves Jr. *et al.* (LHCb Collaboration), The LHCb detector at the LHC, J. Instrum. **3**, S08005 (2008).

[18] R. Aaij *et al.* (LHCb Collaboration), LHCb detector performance, Int. J. Mod. Phys. A **30**, 1530022 (2015).

[19] R. Aaij *et al.*, Performance of the LHCb vertex locator, J. Instrum. **9**, P09007 (2014).

[20] R. Arink *et al.*, Performance of the LHCb outer tracker, J. Instrum. **9**, P01002 (2014).

[21] P. d'Argent *et al.*, Improved performance of the LHCb outer tracker in LHC run 2, J. Instrum. **12**, P11016 (2017).

[22] M. Adinolfi *et al.*, Performance of the LHCb RICH detector at the LHC, Eur. Phys. J. C **73**, 2431 (2013).

[23] A. A. Alves Jr. *et al.*, Performance of the LHCb muon system, J. Instrum. **8**, P02022 (2013).

[24] R. Aaij *et al.*, The LHCb trigger and its performance in 2011, J. Instrum. **8**, P04022 (2013).

[25] V. V. Gligorov and M. Williams, Efficient, reliable and fast high-level triggering using a bonsai boosted decision tree, J. Instrum. **8**, P02013 (2013).

[26] T. Likhomanenko, P. Ilten, E. Khairullin, A. Rogozhnikov, A. Ustyuzhanin, and M. Williams, LHCb topological trigger reoptimization, J. Phys. Conf. Ser. **664**, 082025 (2015).

[27] T. Sjöstrand, S. Mrenna, and P. Skands, A brief introduction to PYTHIA 8.1, Comput. Phys. Commun. **178**, 852 (2008); PYTHIA 6.4 physics and manual, J. High Energy Phys. 05 (2006) 026.

[28] I. Belyaev *et al.*, Handling of the generation of primary events in Gauss, the LHCb simulation framework, J. Phys. Conf. Ser. **331**, 032047 (2011).

[29] D. J. Lange, The EvtGen particle decay simulation package, Nucl. Instrum. Methods Phys. Res., Sect. A **462**, 152 (2001).

[30] N. Davidson, T. Przedzinski, and Z. Was, PHOTOS interface in C++: Technical and physics documentation, Comput. Phys. Commun. **199**, 86 (2016).

[31] J. Allison *et al.* (Geant4 Collaboration), Geant4 developments and applications, IEEE Trans. Nucl. Sci. **53**, 270 (2006); S. Agostinelli *et al.* (Geant4 Collaboration), Geant4: A simulation toolkit, Nucl. Instrum. Methods Phys. Res., Sect. A **506**, 250 (2003).

[32] M. Clemencic, G. Corti, S. Easo, C. R. Jones, S. Miglioranzi, M. Pappagallo, and P. Robbe, The LHCb simulation application, Gauss: Design, evolution and experience, J. Phys. Conf. Ser. **331**, 032023 (2011).

[33] L. Breiman, J. Friedman, R. A. Olshen, and C. J. Stone, *Classification and regression trees* (Chapman and Hall/CRC, 1984).

[34] D. Martínez Santos and F. Dupertuis, Mass distributions marginalized over per-event errors, Nucl. Instrum. Methods Phys. Res., Sect. A **764**, 150 (2014).

[35] T. Skwarnicki, A study of the radiative cascade transitions between the Upsilon-prime and Upsilon resonances, Ph.D. thesis, Institute of Nuclear Physics, Krakow, 1986 [Report No. DESY-F31-86-02].

[36] M. Pivk and F. R. Le Diberder, sPlot: A statistical tool to unfold data distributions, Nucl. Instrum. Methods Phys. Res., Sect. A **555**, 356 (2005).

R. Aaij,[32] A. S. W. Abdelmotteleb,[50] C. Abellan Beteta,[44] F. Abudinén,[50] T. Ackernley,[54] B. Adeva,[40] M. Adinolfi,[48] H. Afsharnia,[9] C. Agapopoulou,[13] C. A. Aidala,[76] S. Aiola,[25] Z. Ajaltouni,[9] S. Akar,[59] K. Akiba,[32] J. Albrecht,[15] F. Alessio,[42] M. Alexander,[53] A. Alfonso Albero,[39] Z. Aliouche,[56] P. Alvarez Cartelle,[49] S. Amato,[2] J. L. Amey,[48] Y. Amhis,[11,42] L. An,[42] L. Anderlini,[22] M. Andersson,[44] A. Andreianov,[38]

M. Andreotti,[21] D. Andreou,[62] D. Ao,[6] F. Archilli,[17] A. Artamonov,[38] M. Artuso,[62] E. Aslanides,[10]
M. Atzeni,[44] B. Audurier,[12] S. Bachmann,[17] M. Bachmayer,[43] J. J. Back,[50] A. Bailly-reyre,[13]
P. Baladron Rodriguez,[40] V. Balagura,[12] W. Baldini,[21] J. Baptista de Souza Leite,[1] M. Barbetti,[22,b] R. J. Barlow,[56]
S. Barsuk,[11] W. Barter,[55] M. Bartolini,[49] F. Baryshnikov,[38] J. M. Basels,[14] G. Bassi,[29,c] B. Batsukh,[4]
A. Battig,[15] A. Bay,[43] A. Beck,[50] M. Becker,[15] F. Bedeschi,[29] I. B. Bediaga,[1] A. Beiter,[62] V. Belavin,[38]
S. Belin,[40] V. Bellee,[44] K. Belous,[38] I. Belov,[38] I. Belyaev,[38] G. Bencivenni,[23] E. Ben-Haim,[13]
A. Berezhnoy,[38] R. Bernet,[44] D. Berninghoff,[17] H. C. Bernstein,[62] C. Bertella,[56] A. Bertolin,[28] C. Betancourt,[44]
F. Betti,[42] Ia. Bezshyiko,[44] S. Bhasin,[48] J. Bhom,[35] L. Bian,[67] M. S. Bieker,[15] N. V. Biesuz,[21] S. Bifani,[47]
P. Billoir,[13] A. Biolchini,[32] M. Birch,[55] F. C. R. Bishop,[49] A. Bitadze,[56] A. Bizzeti, M. Bjørn,[57] M. P. Blago,[49]
T. Blake,[50] F. Blanc,[43] S. Blusk,[62] D. Bobulska,[53] J. A. Boelhauve,[15] O. Boente Garcia,[40] T. Boettcher,[59]
A. Boldyrev,[38] N. Bondar,[38,42] S. Borghi,[56] M. Borsato,[17] J. T. Borsuk,[35] S. A. Bouchiba,[43]
T. J. V. Bowcock,[54,42] A. Boyer,[42] C. Bozzi,[21] M. J. Bradley,[55] S. Braun,[60] A. Brea Rodriguez,[40] J. Brodzicka,[35]
A. Brossa Gonzalo,[50] D. Brundu,[27] A. Buonaura,[44] L. Buonincontri,[28] A. T. Burke,[56] C. Burr,[42] A. Bursche,[66]
A. Butkevich,[38] J. S. Butter,[32] J. Buytaert,[42] W. Byczynski,[42] S. Cadeddu,[27] H. Cai,[67] R. Calabrese,[21,d]
L. Calefice,[15,13] S. Cali,[23] R. Calladine,[47] M. Calvi,[26,e] M. Calvo Gomez,[74] P. Camargo Magalhaes,[48]
P. Campana,[23] D. H. Campora Perez,[73] A. F. Campoverde Quezada,[6] S. Capelli,[26,e] L. Capriotti,[20,f]
A. Carbone,[20,f] G. Carboni,[31] R. Cardinale,[24,g] A. Cardini,[27] I. Carli,[4] P. Carniti,[26,e] L. Carus,[14]
A. Casais Vidal,[40] R. Caspary,[17] G. Casse,[54] M. Cattaneo,[42] G. Cavallero,[42] V. Cavallini,[21,d] S. Celani,[43]
J. Cerasoli,[10] D. Cervenkov,[57] A. J. Chadwick,[54] M. G. Chapman,[48] M. Charles,[13] Ph. Charpentier,[42]
C. A. Chavez Barajas,[54] M. Chefdeville,[8] C. Chen,[3] S. Chen,[4] A. Chernov,[35] S. Chernyshenko,[46]
V. Chobanova,[40] S. Cholak,[43] M. Chrzaszcz,[35] A. Chubykin,[38] V. Chulikov,[38] P. Ciambrone,[23] M. F. Cicala,[50]
X. Cid Vidal,[40] G. Ciezarek,[42] G. Ciullo,[21,d] P. E. L. Clarke,[52] M. Clemencic,[42] H. V. Cliff,[49] J. Closier,[42]
J. L. Cobbledick,[56] V. Coco,[42] J. A. B. Coelho,[11] J. Cogan,[10] E. Cogneras,[9] L. Cojocariu,[37] P. Collins,[42]
T. Colombo,[42] L. Congedo,[19,h] A. Contu,[27] N. Cooke,[47] G. Coombs,[53] I. Corredoira,[40] G. Corti,[42]
B. Couturier,[42] D. C. Craik,[58] J. Crkovská,[61] M. Cruz Torres,[1,i] R. Currie,[52] C. L. Da Silva,[61] S. Dadabaev,[38]
L. Dai,[65] E. Dall'Occo,[15] J. Dalseno,[40] C. D'Ambrosio,[42] A. Danilina,[38] P. d'Argent,[15] J. E. Davies,[56]
A. Davis,[56] O. De Aguiar Francisco,[56] J. de Boer,[42] K. De Bruyn,[72] S. De Capua,[56] M. De Cian,[43]
U. De Freitas Carneiro Da Graca,[1] E. De Lucia,[23] J. M. De Miranda,[1] L. De Paula,[2] M. De Serio,[19,h]
D. De Simone,[44] P. De Simone,[23] F. De Vellis,[15] J. A. de Vries,[73] C. T. Dean,[61] F. Debernardis,[19,h] D. Decamp,[8]
V. Dedu,[10] L. Del Buono,[13] B. Delaney,[49] H.-P. Dembinski,[15] V. Denysenko,[44] O. Deschamps,[9] F. Dettori,[27,j]
B. Dey,[70] A. Di Cicco,[23] P. Di Nezza,[23] S. Didenko,[38] L. Dieste Maronas,[40] S. Ding,[62] V. Dobishuk,[46]
A. Dolmatov,[38] C. Dong,[3] A. M. Donohoe,[18] F. Dordei,[27] A. C. dos Reis,[1] L. Douglas,[53] A. G. Downes,[8]
M. W. Dudek,[35] L. Dufour,[42] V. Duk,[71] P. Durante,[42] J. M. Durham,[61] D. Dutta,[56] A. Dziurda,[35] A. Dzyuba,[38]
S. Easo,[51] U. Egede,[63] V. Egorychev,[38] S. Eidelman,[38,a] S. Eisenhardt,[52] S. Ek-In,[43] L. Eklund,[75] S. Ely,[62]
A. Ene,[37] E. Epple,[61] S. Escher,[14] J. Eschle,[44] S. Esen,[44] T. Evans,[56] L. N. Falcao,[1] Y. Fan,[6] B. Fang,[67]
S. Farry,[54] D. Fazzini,[26,e] M. Feo,[42] A. D. Fernez,[60] F. Ferrari,[20] L. Ferreira Lopes,[43] F. Ferreira Rodrigues,[2]
S. Ferreres Sole,[32] M. Ferrillo,[44] M. Ferro-Luzzi,[42] S. Filippov,[38] R. A. Fini,[19] M. Fiorini,[21,d] M. Firlej,[34]
K. M. Fischer,[57] D. S. Fitzgerald,[76] C. Fitzpatrick,[56] T. Fiutowski,[34] F. Fleuret,[12] M. Fontana,[13] F. Fontanelli,[24,g]
R. Forty,[42] D. Foulds-Holt,[49] V. Franco Lima,[54] M. Franco Sevilla,[60] M. Frank,[42] E. Franzoso,[21,d] G. Frau,[17]
C. Frei,[42] D. A. Friday,[53] J. Fu,[6] Q. Fuehring,[15] E. Gabriel,[32] G. Galati,[19,h] A. Gallas Torreira,[40] D. Galli,[20,f]
S. Gambetta,[52,42] Y. Gan,[3] M. Gandelman,[2] P. Gandini,[25] Y. Gao,[5] M. Garau,[27,j] L. M. Garcia Martin,[50]
P. Garcia Moreno,[39] J. García Pardiñas,[26,e] B. Garcia Plana,[40] F. A. Garcia Rosales,[12] L. Garrido,[39] C. Gaspar,[42]
R. E. Geertsema,[32] D. Gerick,[17] L. L. Gerken,[15] E. Gersabeck,[56] M. Gersabeck,[56] T. Gershon,[50]
L. Giambastiani,[28] V. Gibson,[49] H. K. Giemza,[36] A. L. Gilman,[57] M. Giovannetti,[23,k] A. Gioventù,[40]
P. Gironella Gironell,[39] C. Giugliano,[21,d] K. Gizdov,[52] E. L. Gkougkousis,[42] V. V. Gligorov,[13,42] C. Göbel,[64]
E. Golobardes,[74] D. Golubkov,[38] A. Golutvin,[55,38] A. Gomes,[1,l] S. Gomez Fernandez,[39] F. Goncalves Abrantes,[57]
M. Goncerz,[35] G. Gong,[3] I. V. Gorelov,[38] C. Gotti,[26] J. P. Grabowski,[17] T. Grammatico,[13]
L. A. Granado Cardoso,[42] E. Graugés,[39] E. Graverini,[43] G. Graziani, A. T. Grecu,[37] L. M. Greeven,[32]
N. A. Grieser,[4] L. Grillo,[53] S. Gromov,[38] B. R. Gruberg Cazon,[57] C. Gu,[3] M. Guarise,[21,d] M. Guittiere,[11]

P. A. Günther,[17] E. Gushchin,[38] A. Guth,[14] Y. Guz,[38] T. Gys,[42] T. Hadavizadeh,[63] G. Haefeli,[43] C. Haen,[42]
J. Haimberger,[42] S. C. Haines,[49] T. Halewood-leagas,[54] M. M. Halvorsen,[42] P. M. Hamilton,[60] J. Hammerich,[54]
Q. Han,[7] X. Han,[17] E. B. Hansen,[56] S. Hansmann-Menzemer,[17,42] L. Hao,[6] N. Harnew,[57] T. Harrison,[54]
C. Hasse,[42] M. Hatch,[42] J. He,[6,m] K. Heijhoff,[32] K. Heinicke,[15] R. D. L. Henderson,[63,50] A. M. Hennequin,[58]
K. Hennessy,[54] L. Henry,[42] J. Heuel,[14] A. Hicheur,[2] D. Hill,[43] M. Hilton,[56] S. E. Hollitt,[15] R. Hou,[7] Y. Hou,[8]
J. Hu,[17] J. Hu,[66] W. Hu,[7] X. Hu,[3] W. Huang,[6] X. Huang,[67] W. Hulsbergen,[32] R. J. Hunter,[50] M. Hushchyn,[38]
D. Hutchcroft,[54] P. Ibis,[15] M. Idzik,[34] D. Ilin,[38] P. Ilten,[59] A. Inglessi,[38] A. Iniukhin,[38] A. Ishteev,[38]
K. Ivshin,[38] R. Jacobsson,[42] H. Jage,[14] S. Jakobsen,[42] E. Jans,[32] B. K. Jashal,[41] A. Jawahery,[60] V. Jevtic,[15]
X. Jiang,[4,6] M. John,[57] D. Johnson,[58] C. R. Jones,[49] T. P. Jones,[50] B. Jost,[42] N. Jurik,[42] S. Kandybei,[45]
Y. Kang,[3] M. Karacson,[42] D. Karpenkov,[38] M. Karpov,[38] J. W. Kautz,[59] F. Keizer,[42] D. M. Keller,[62]
M. Kenzie,[50] T. Ketel,[33] B. Khanji,[15] A. Kharisova,[38] S. Kholodenko,[38] T. Kirn,[14] V. S. Kirsebom,[43]
O. Kitouni,[58] S. Klaver,[33] N. Kleijne,[29,c] K. Klimaszewski,[36] M. R. Kmiec,[36] S. Koliiev,[46] A. Kondybayeva,[38]
A. Konoplyannikov,[38] P. Kopciewicz,[34] R. Kopecna,[17] P. Koppenburg,[32] M. Korolev,[38] I. Kostiuk,[32,46] O. Kot,[46]
S. Kotriakhova, A. Kozachuk,[38] P. Kravchenko,[38] L. Kravchuk,[38] R. D. Krawczyk,[42] M. Kreps,[50]
S. Kretzschmar,[14] P. Krokovny,[38] W. Krupa,[34] W. Krzemien,[36] J. Kubat,[17] W. Kucewicz,[35,34] M. Kucharczyk,[35]
V. Kudryavtsev,[38] H. S. Kuindersma,[32] G. J. Kunde,[61] D. Lacarrere,[42] G. Lafferty,[56] A. Lai,[27] A. Lampis,[27,j]
D. Lancierini,[44] J. J. Lane,[56] R. Lane,[48] G. Lanfranchi,[23] C. Langenbruch,[14] J. Langer,[15] O. Lantwin,[38]
T. Latham,[50] F. Lazzari,[29,n] M. Lazzaroni,[25,o] R. Le Gac,[10] S. H. Lee,[76] R. Lefèvre,[9] A. Leflat,[38] S. Legotin,[38]
P. Lenisa,[21,d] O. Leroy,[10] T. Lesiak,[35] B. Leverington,[17] H. Li,[66] K. Li,[7] P. Li,[17] S. Li,[7] Y. Li,[4] Z. Li,[62]
X. Liang,[62] C. Lin,[6] T. Lin,[55] R. Lindner,[42] V. Lisovskyi,[15] R. Litvinov,[27,j] G. Liu,[66] H. Liu,[6] Q. Liu,[6]
S. Liu,[4,6] A. Lobo Salvia,[39] A. Loi,[27] R. Lollini,[71] J. Lomba Castro,[40] I. Longstaff,[53] J. H. Lopes,[2]
S. López Soliño,[40] G. H. Lovell,[49] Y. Lu,[4,p] C. Lucarelli,[22,b] D. Lucchesi,[28,q] S. Luchuk,[38] M. Lucio Martinez,[32]
V. Lukashenko,[32,46] Y. Luo,[3] A. Lupato,[56] E. Luppi,[21,d] A. Lusiani,[29,c] K. Lynch,[18] X.-R. Lyu,[6] L. Ma,[4]
R. Ma,[6] S. Maccolini,[20] F. Machefert,[11] F. Maciuc,[37] V. Macko,[43] P. Mackowiak,[15] S. Maddrell-Mander,[48]
L. R. Madhan Mohan,[48] A. Maevskiy,[38] D. Maisuzenko,[38] M. W. Majewski,[34] J. J. Malczewski,[35] S. Malde,[57]
B. Malecki,[35] A. Malinin,[38] T. Maltsev,[38] H. Malygina,[17] G. Manca,[27,j] G. Mancinelli,[10] D. Manuzzi,[20]
C. A. Manzari,[44] D. Marangotto,[25,o] J. F. Marchand,[8] U. Marconi,[20] S. Mariani,[22,b] C. Marin Benito,[42]
M. Marinangeli,[43] J. Marks,[17] A. M. Marshall,[48] P. J. Marshall,[54] G. Martelli,[71,r] G. Martellotti,[30]
L. Martinazzoli,[42,e] M. Martinelli,[26,e] D. Martinez Santos,[40] F. Martinez Vidal,[41] A. Massafferri,[1] M. Materok,[14]
R. Matev,[42] A. Mathad,[44] V. Matiunin,[38] C. Matteuzzi,[26] K. R. Mattioli,[76] A. Mauri,[32] E. Maurice,[12]
J. Mauricio,[39] M. Mazurek,[42] M. McCann,[55] L. Mcconnell,[18] T. H. McGrath,[56] N. T. McHugh,[53] A. McNab,[56]
R. McNulty,[18] J. V. Mead,[54] B. Meadows,[59] G. Meier,[15] D. Melnychuk,[36] S. Meloni,[26,e] M. Merk,[32,73]
A. Merli,[25,o] L. Meyer Garcia,[2] M. Mikhasenko,[69,s] D. A. Milanes,[68] E. Millard,[50] M. Milovanovic,[42]
M.-N. Minard,[8,a] A. Minotti,[26,e] S. E. Mitchell,[52] B. Mitreska,[56] D. S. Mitzel,[15] A. Mödden,[15]
R. A. Mohammed,[57] R. D. Moise,[55] S. Mokhnenko,[38] T. Mombächer,[40] I. A. Monroy,[68] S. Monteil,[9]
M. Morandin,[28] G. Morello,[23] M. J. Morello,[29,c] J. Moron,[34] A. B. Morris,[69] A. G. Morris,[50] R. Mountain,[62]
H. Mu,[3] F. Muheim,[52] M. Mulder,[72] K. Müller,[44] C. H. Murphy,[57] D. Murray,[56] R. Murta,[55] P. Muzzetto,[27,j]
P. Naik,[48] T. Nakada,[43] R. Nandakumar,[51] T. Nanut,[42] I. Nasteva,[2] M. Needham,[52] N. Neri,[25,o] S. Neubert,[69]
N. Neufeld,[42] P. Neustroev,[38] R. Newcombe,[55] E. M. Niel,[43] S. Nieswand,[14] N. Nikitin,[38] N. S. Nolte,[58]
C. Normand,[8,27,j] C. Nunez,[76] A. Oblakowska-Mucha,[34] V. Obraztsov,[38] T. Oeser,[14] D. P. O'Hanlon,[48]
S. Okamura,[21,d] R. Oldeman,[27,j] F. Oliva,[52] M. E. Olivares,[62] C. J. G. Onderwater,[72] R. H. O'Neil,[52]
J. M. Otalora Goicochea,[2] T. Ovsiannikova,[38] P. Owen,[44] A. Oyanguren,[41] O. Ozcelik,[52] K. O. Padeken,[69]
B. Pagare,[50] P. R. Pais,[42] T. Pajero,[57] A. Palano,[19] M. Palutan,[23] Y. Pan,[56] G. Panshin,[38] A. Papanestis,[51]
M. Pappagallo,[19,h] L. L. Pappalardo,[21,d] C. Pappenheimer,[59] W. Parker,[60] C. Parkes,[56] B. Passalacqua,[21,d]
G. Passaleva,[22] A. Pastore,[19] M. Patel,[55] C. Patrignani,[20,f] C. J. Pawley,[73] A. Pearce,[42] A. Pellegrino,[32]
M. Pepe Altarelli,[42] S. Perazzini,[20] D. Pereima,[38] A. Pereiro Castro,[40] P. Perret,[9] M. Petric,[53] K. Petridis,[48]
A. Petrolini,[24,g] A. Petrov,[38] S. Petrucci,[52] M. Petruzzo,[25] H. Pham,[62] A. Philippov,[38] R. Piandani,[6] L. Pica,[29,c]
M. Piccini,[71] B. Pietrzyk,[8] G. Pietrzyk,[11] M. Pili,[57] D. Pinci,[30] F. Pisani,[42] M. Pizzichemi,[26,42,e] V. Placinta,[37]
J. Plews,[47] M. Plo Casasus,[40] F. Polci,[13,42] M. Poli Lener,[23] M. Poliakova,[62] A. Poluektov,[10] N. Polukhina,[38]

I. Polyakov,[62] E. Polycarpo,[2] S. Ponce,[42] D. Popov,[6,42] S. Popov,[38] S. Poslavskii,[38] K. Prasanth,[35] L. Promberger,[42] C. Prouve,[40] V. Pugatch,[46] V. Puill,[11] G. Punzi,[29,t] H. R. Qi,[3] W. Qian,[6] N. Qin,[3] S. Qu,[3] R. Quagliani,[43] N. V. Raab,[18] R. I. Rabadan Trejo,[6] B. Rachwal,[34] J. H. Rademacker,[48] R. Rajagopalan,[62] M. Rama,[29] M. Ramos Pernas,[50] M. S. Rangel,[2] F. Ratnikov,[38] G. Raven,[33,42] M. Rebollo De Miguel,[41] M. Reboud,[8] F. Redi,[42] F. Reiss,[56] C. Remon Alepuz,[41] Z. Ren,[3] V. Renaudin,[57] P. K. Resmi,[10] R. Ribatti,[29,c] A. M. Ricci,[27] S. Ricciardi,[51] K. Rinnert,[54] P. Robbe,[11] G. Robertson,[52] A. B. Rodrigues,[43] E. Rodrigues,[54] J. A. Rodriguez Lopez,[68] E. Rodriguez Rodriguez,[40] A. Rollings,[57] P. Roloff,[42] V. Romanovskiy,[38] M. Romero Lamas,[40] A. Romero Vidal,[40] J. D. Roth,[76,a] M. Rotondo,[23] M. S. Rudolph,[62] T. Ruf,[42] R. A. Ruiz Fernandez,[40] J. Ruiz Vidal,[41] A. Ryzhikov,[38] J. Ryzka,[34] J. J. Saborido Silva,[40] N. Sagidova,[38] N. Sahoo,[47] B. Saitta,[27,j] M. Salomoni,[42] C. Sanchez Gras,[32] I. Sanderswood,[41] R. Santacesaria,[30] C. Santamarina Rios,[40] M. Santimaria,[23] E. Santovetti,[31,k] D. Saranin,[38] G. Sarpis,[14] M. Sarpis,[69] A. Sarti,[30] C. Satriano,[30,u] A. Satta,[31] M. Saur,[15] D. Savrina,[38] H. Sazak,[9] L. G. Scantlebury Smead,[57] A. Scarabotto,[13] S. Schael,[14] S. Scherl,[54] M. Schiller,[53] H. Schindler,[42] M. Schmelling,[16] B. Schmidt,[42] S. Schmitt,[14] O. Schneider,[43] A. Schopper,[42] M. Schubiger,[32] S. Schulte,[43] M. H. Schune,[11] R. Schwemmer,[42] B. Sciascia,[23,42] A. Sciuccati,[42] S. Sellam,[40] A. Semennikov,[38] M. Senghi Soares,[33] A. Sergi,[24,g] N. Serra,[44] L. Sestini,[28] A. Seuthe,[15] Y. Shang,[5] D. M. Shangase,[76] M. Shapkin,[38] I. Shchemerov,[38] L. Shchutska,[43] T. Shears,[54] L. Shekhtman,[38] Z. Shen,[5] S. Sheng,[4,6] V. Shevchenko,[38] E. B. Shields,[26,e] Y. Shimizu,[11] E. Shmanin,[38] J. D. Shupperd,[62] B. G. Siddi,[21,d] R. Silva Coutinho,[44] G. Simi,[28] S. Simone,[19,h] M. Singla,[63] N. Skidmore,[56] R. Skuza,[17] T. Skwarnicki,[62] M. W. Slater,[47] I. Slazyk,[21,d] J. C. Smallwood,[57] J. G. Smeaton,[49] E. Smith,[44] M. Smith,[55] A. Snoch,[32] L. Soares Lavra,[9] M. D. Sokoloff,[59] F. J. P. Soler,[53] A. Solomin,[38,48] A. Solovev,[38] I. Solovyev,[38] F. L. Souza De Almeida,[2] B. Souza De Paula,[2] B. Spaan,[15,a] E. Spadaro Norella,[25,o] E. Spiridenkov,[38] P. Spradlin,[53] V. Sriskaran,[42] F. Stagni,[42] M. Stahl,[59] S. Stahl,[42] S. Stanislaus,[57] O. Steinkamp,[44] O. Stenyakin,[38] H. Stevens,[15] S. Stone,[62,a] D. Strekalina,[38] F. Suljik,[57] J. Sun,[27] L. Sun,[67] Y. Sun,[60] P. Svihra,[56] P. N. Swallow,[47] K. Swientek,[34] A. Szabelski,[36] T. Szumlak,[34] M. Szymanski,[42] S. Taneja,[56] A. R. Tanner,[48] M. D. Tat,[57] A. Terentev,[38] F. Teubert,[42] E. Thomas,[42] D. J. D. Thompson,[47] K. A. Thomson,[54] H. Tilquin,[55] V. Tisserand,[9] S. T'Jampens,[8] M. Tobin,[4] L. Tomassetti,[21,d] G. Tonani,[25,o] X. Tong,[5] D. Torres Machado,[1] D. Y. Tou,[3] E. Trifonova,[38] S. M. Trilov,[48] C. Trippl,[43] G. Tuci,[6] A. Tully,[43] N. Tuning,[32,42] A. Ukleja,[36] D. J. Unverzagt,[17] E. Ursov,[38] A. Usachov,[32] A. Ustyuzhanin,[38] U. Uwer,[17] A. Vagner,[38] V. Vagnoni,[20] A. Valassi,[42] G. Valenti,[20] N. Valls Canudas,[74] M. van Beuzekom,[32] M. Van Dijk,[43] H. Van Hecke,[61] E. van Herwijnen,[38] M. van Veghel,[72] R. Vazquez Gomez,[39] P. Vazquez Regueiro,[40] C. Vázquez Sierra,[42] S. Vecchi,[21] J. J. Velthuis,[48] M. Veltri,[22,v] A. Venkateswaran,[62] M. Veronesi,[32] M. Vesterinen,[50] D. Vieira,[59] M. Vieites Diaz,[43] X. Vilasis-Cardona,[74] E. Vilella Figueras,[54] A. Villa,[20] P. Vincent,[13] F. C. Volle,[11] D. vom Bruch,[10] A. Vorobyev,[38] V. Vorobyev,[38] N. Voropaev,[38] K. Vos,[73] R. Waldi,[17] J. Walsh,[29] C. Wang,[17] J. Wang,[5] J. Wang,[4] J. Wang,[3] J. Wang,[67] M. Wang,[5] R. Wang,[48] Y. Wang,[7] Z. Wang,[44] Z. Wang,[3] Z. Wang,[6] J. A. Ward,[50,63] N. K. Watson,[47] D. Websdale,[55] C. Weisser,[58] B. D. C. Westhenry,[48] D. J. White,[56] M. Whitehead,[53] A. R. Wiederhold,[50] D. Wiedner,[15] G. Wilkinson,[57] M. K. Wilkinson,[59] I. Williams,[49] M. Williams,[58] M. R. J. Williams,[52] F. F. Wilson,[51] W. Wislicki,[36] M. Witek,[35] L. Witola,[17] C. P. Wong,[61] G. Wormser,[11] S. A. Wotton,[49] H. Wu,[62] K. Wyllie,[42] Z. Xiang,[6] D. Xiao,[7] Y. Xie,[7] A. Xu,[5] J. Xu,[6] L. Xu,[3] M. Xu,[50] Q. Xu,[6] Z. Xu,[9] Z. Xu,[6] D. Yang,[3] S. Yang,[6] Y. Yang,[6] Z. Yang,[5] Z. Yang,[60] Y. Yao,[62] L. E. Yeomans,[54] H. Yin,[7] J. Yu,[65] X. Yuan,[62] E. Zaffaroni,[43] M. Zavertyaev,[16] M. Zdybal,[35] O. Zenaiev,[42] M. Zeng,[3] D. Zhang,[7] L. Zhang,[3] S. Zhang,[65] S. Zhang,[5] Y. Zhang,[5] Y. Zhang,[57] A. Zharkova,[38] A. Zhelezov,[17] Y. Zheng,[6] T. Zhou,[5] X. Zhou,[6] Y. Zhou,[6] V. Zhovkovska,[11] X. Zhu,[3] X. Zhu,[7] Z. Zhu,[6] V. Zhukov,[14,38] Q. Zou,[4,6] S. Zucchelli,[20,f] D. Zuliani,[28] and G. Zunica[56]

(LHCb Collaboration)

[1]*Centro Brasileiro de Pesquisas Físicas (CBPF), Rio de Janeiro, Brazil*
[2]*Universidade Federal do Rio de Janeiro (UFRJ), Rio de Janeiro, Brazil*
[3]*Center for High Energy Physics, Tsinghua University, Beijing, China*
[4]*Institute Of High Energy Physics (IHEP), Beijing, China*

[5]*School of Physics State Key Laboratory of Nuclear Physics and Technology, Peking University, Beijing, China*
[6]*University of Chinese Academy of Sciences, Beijing, China*
[7]*Institute of Particle Physics, Central China Normal University, Wuhan, Hubei, China*
[8]*Université Savoie Mont Blanc, CNRS, IN2P3-LAPP, Annecy, France*
[9]*Université Clermont Auvergne, CNRS/IN2P3, LPC, Clermont-Ferrand, France*
[10]*Aix Marseille Univ, CNRS/IN2P3, CPPM, Marseille, France*
[11]*Université Paris-Saclay, CNRS/IN2P3, IJCLab, Orsay, France*
[12]*Laboratoire Leprince-Ringuet, CNRS/IN2P3, Ecole Polytechnique, Institut Polytechnique de Paris, Palaiseau, France*
[13]*LPNHE, Sorbonne Université, Paris Diderot Sorbonne Paris Cité, CNRS/IN2P3, Paris, France*
[14]*I. Physikalisches Institut, RWTH Aachen University, Aachen, Germany*
[15]*Fakultät Physik, Technische Universität Dortmund, Dortmund, Germany*
[16]*Max-Planck-Institut für Kernphysik (MPIK), Heidelberg, Germany*
[17]*Physikalisches Institut, Ruprecht-Karls-Universität Heidelberg, Heidelberg, Germany*
[18]*School of Physics, University College Dublin, Dublin, Ireland*
[19]*INFN Sezione di Bari, Bari, Italy*
[20]*INFN Sezione di Bologna, Bologna, Italy*
[21]*INFN Sezione di Ferrara, Ferrara, Italy*
[22]*INFN Sezione di Firenze, Firenze, Italy*
[23]*INFN Laboratori Nazionali di Frascati, Frascati, Italy*
[24]*INFN Sezione di Genova, Genova, Italy*
[25]*INFN Sezione di Milano, Milano, Italy*
[26]*INFN Sezione di Milano-Bicocca, Milano, Italy*
[27]*INFN Sezione di Cagliari, Monserrato, Italy*
[28]*Università degli Studi di Padova, Università e INFN, Padova, Padova, Italy*
[29]*INFN Sezione di Pisa, Pisa, Italy*
[30]*INFN Sezione di Roma La Sapienza, Roma, Italy*
[31]*INFN Sezione di Roma Tor Vergata, Roma, Italy*
[32]*Nikhef National Institute for Subatomic Physics, Amsterdam, Netherlands*
[33]*Nikhef National Institute for Subatomic Physics and VU University Amsterdam, Amsterdam, Netherlands*
[34]*AGH - University of Science and Technology, Faculty of Physics and Applied Computer Science, Kraków, Poland*
[35]*Henryk Niewodniczanski Institute of Nuclear Physics Polish Academy of Sciences, Kraków, Poland*
[36]*National Center for Nuclear Research (NCBJ), Warsaw, Poland*
[37]*Horia Hulubei National Institute of Physics and Nuclear Engineering, Bucharest-Magurele, Romania*
[38]*Affiliated with an institute covered by a cooperation agreement with CERN*
[39]*ICCUB, Universitat de Barcelona, Barcelona, Spain*
[40]*Instituto Galego de Física de Altas Enerxías (IGFAE), Universidade de Santiago de Compostela, Santiago de Compostela, Spain*
[41]*Instituto de Fisica Corpuscular, Centro Mixto Universidad de Valencia—CSIC, Valencia, Spain*
[42]*European Organization for Nuclear Research (CERN), Geneva, Switzerland*
[43]*Institute of Physics, Ecole Polytechnique Fédérale de Lausanne (EPFL), Lausanne, Switzerland*
[44]*Physik-Institut, Universität Zürich, Zürich, Switzerland*
[45]*NSC Kharkiv Institute of Physics and Technology (NSC KIPT), Kharkiv, Ukraine*
[46]*Institute for Nuclear Research of the National Academy of Sciences (KINR), Kyiv, Ukraine*
[47]*University of Birmingham, Birmingham, United Kingdom*
[48]*H.H. Wills Physics Laboratory, University of Bristol, Bristol, United Kingdom*
[49]*Cavendish Laboratory, University of Cambridge, Cambridge, United Kingdom*
[50]*Department of Physics, University of Warwick, Coventry, United Kingdom*
[51]*STFC Rutherford Appleton Laboratory, Didcot, United Kingdom*
[52]*School of Physics and Astronomy, University of Edinburgh, Edinburgh, United Kingdom*
[53]*School of Physics and Astronomy, University of Glasgow, Glasgow, United Kingdom*
[54]*Oliver Lodge Laboratory, University of Liverpool, Liverpool, United Kingdom*
[55]*Imperial College London, London, United Kingdom*
[56]*Department of Physics and Astronomy, University of Manchester, Manchester, United Kingdom*
[57]*Department of Physics, University of Oxford, Oxford, United Kingdom*
[58]*Massachusetts Institute of Technology, Cambridge, MA, United States*
[59]*University of Cincinnati, Cincinnati, OH, United States*
[60]*University of Maryland, College Park, MD, United States*

[61]*Los Alamos National Laboratory (LANL), Los Alamos, NM, United States*
[62]*Syracuse University, Syracuse, NY, United States*
[63]*School of Physics and Astronomy, Monash University, Melbourne, Australia (associated with Department of Physics, University of Warwick, Coventry, United Kingdom)*
[64]*Pontifícia Universidade Católica do Rio de Janeiro (PUC-Rio), Rio de Janeiro, Brazil (associated with Universidade Federal do Rio de Janeiro (UFRJ), Rio de Janeiro, Brazil)*
[65]*Physics and Micro Electronic College, Hunan University, Changsha City, China (associated with Institute of Particle Physics, Central China Normal University, Wuhan, Hubei, China)*
[66]*Guangdong Provincial Key Laboratory of Nuclear Science, Guangdong-Hong Kong Joint Laboratory of Quantum Matter, Institute of Quantum Matter, South China Normal University, Guangzhou, China (associated with Center for High Energy Physics, Tsinghua University, Beijing, China)*
[67]*School of Physics and Technology, Wuhan University, Wuhan, China (associated with Center for High Energy Physics, Tsinghua University, Beijing, China)*
[68]*Departamento de Fisica, Universidad Nacional de Colombia, Bogota, Colombia (associated with LPNHE, Sorbonne Université, Paris Diderot Sorbonne Paris Cité, CNRS/IN2P3, Paris, France)*
[69]*Universität Bonn-Helmholtz-Institut für Strahlen und Kernphysik, Bonn, Germany (associated with Physikalisches Institut, Ruprecht-Karls-Universität Heidelberg, Heidelberg, Germany)*
[70]*Eotvos Lorand University, Budapest, Hungary (associated with European Organization for Nuclear Research (CERN), Geneva, Switzerland)*
[71]*INFN Sezione di Perugia, Perugia, Italy (associated with INFN Sezione di Ferrara, Ferrara, Italy)*
[72]*Van Swinderen Institute, University of Groningen, Groningen, Netherlands (associated with Nikhef National Institute for Subatomic Physics, Amsterdam, Netherlands)*
[73]*Universiteit Maastricht, Maastricht, Netherlands (associated with Nikhef National Institute for Subatomic Physics, Amsterdam, Netherlands)*
[74]*DS4DS, La Salle, Universitat Ramon Llull, Barcelona, Spain (associated with ICCUB, Universitat de Barcelona, Barcelona, Spain)*
[75]*Department of Physics and Astronomy, Uppsala University, Uppsala, Sweden (associated with School of Physics and Astronomy, University of Glasgow, Glasgow, United Kingdom)*
[76]*University of Michigan, Ann Arbor, Michigan, USA (associated with Syracuse University, Syracuse, New York, USA)*

[a] Deceased.
[b] Also at Università di Firenze, Firenze, Italy.
[c] Also at Scuola Normale Superiore, Pisa, Italy.
[d] Also at Università di Ferrara, Ferrara, Italy.
[e] Also at Università di Milano Bicocca, Milano, Italy.
[f] Also at Università di Bologna, Bologna, Italy.
[g] Also at Università di Genova, Genova, Italy.
[h] Also at Università di Bari, Bari, Italy.
[i] Also at Universidad Nacional Autónoma de Honduras, Tegucigalpa, Honduras.
[j] Also at Università di Cagliari, Cagliari, Italy.
[k] Also at Università di Roma Tor Vergata, Roma, Italy.
[l] Also at Universidade Federal do Triângulo Mineiro (UFTM), Uberaba-MG, Brazil.
[m] Also at Hangzhou Institute for Advanced Study, UCAS, Hangzhou, China.
[n] Also at Università di Siena, Siena, Italy.
[o] Also at Università degli Studi di Milano, Milano, Italy.
[p] Also at Central South University, Changsha, China.
[q] Also at Università di Padova, Padova, Italy.
[r] Also at Università di Perugia, Perugia, Italy.
[s] Also at Excellence Cluster ORIGINS, Munich, Germany.
[t] Also at Università di Pisa, Pisa, Italy.
[u] Also at Università della Basilicata, Potenza, Italy.
[v] Also at Università di Urbino, Urbino, Italy.